

# Effect of structural defects on optical properties of amorphous selenium films

M. F. KOTKATA, F. A. ABDEL-WAHAB

*Physics Department, Faculty of Science, Ain Shams University, Cairo, Egypt*

Thickness of film, energy of incident photons and glass transition temperature all affect the structural bonding between neighbours and are considered to be the main factors in studying the optical properties of amorphous selenium films. The results indicate that in the low-temperature range ( $T < T_g$ ), a shift in the absorption edge to lower photon energies with increasing film thickness occurs. Increasing the thickness is accompanied by a decrease in the optical energy gap,  $E_g^{\text{opt}}$ , with a gradient of  $5 \times 10^{-4} \text{ eV nm}^{-1}$ . In the high-temperature range ( $T > T_g$ ), the value of  $E_g^{\text{opt}}$  for a given thickness decreases by more than 50% due to pronounced modulation of the structural defects under incidence of isoenergetic photons of 1.8 eV. The isothermal curves of  $T, R = f(t)$ , at  $T > T_g$ , take place via three time-dependent stages. These results are interpreted and are correlated with the temperature dependence of the morphological changes declaring the formation of spherulites having a lamellar structure. The kinetic parameters controlling the structural transition are computed and the results are discussed.

## 1. Introduction

Various properties of amorphous selenium (a-Se) have been studied including photo- or thermo-crystallization. Selenyi [1, 2] observed that light enhances the crystallization of a-Se at lower temperature. Changes with illumination in the morphology and growth rate of selenium crystals grown from the vapour phase have been observed and ascribed to thermal effects [3]. An increase in the growth velocity of individual selenium crystallites under irradiation by a neon light at 130°C has also been reported [4]. Dresner and Stringfellow [5], demonstrated that the increase of the crystal growth rate by light results from the production of hole–electron pairs in the a-Se and that the growth is controlled by the flux of holes towards the crystal boundary. Moreover, Ovshinsky and Klose [6] have shown that the number of nuclei can be greatly increased by light (photonucleation), specially in films sensitized by the incorporation of certain crystals. The nuclei can then be developed through subsequent grain growth either thermally or in combination with light [7].

A chalcogen such as selenium exhibits divalent bonding and the structural stability is one-dimensional in nature (chain-like structure) [8]. The structural bonding between neighbours determines the optical properties, such as absorption and transmission, of the amorphous material. However, a continuous recording for the variation of the optical constants during the amorphous-to-crystalline (a–c) transition of selenium films has not yet been reported.

In the present study, the spectral distribution curves of a-Se films have been studied and the optical parameters, e.g. refractive index ( $n$ ), the absorption coefficient ( $\alpha$ ) and energy gap ( $E_g^{\text{opt}}$ ), have been calculated

for different film thicknesses ( $d$ ). Also, the continuous variation of  $n$  and  $\alpha$  has been recorded as a function of time ( $t$ ) at different isotherms ( $T_c$ ) in the range 70 to 120°C. The data obtained are used to calculate the kinetic parameters of the crystallization process together with the morphological changes of selenium growth.

## 2. Experimental methods

Elemental selenium with purity 99.9999% was used as a starting material. Selenium films of different thicknesses were thermally deposited under a vacuum of  $10^{-5}$  torr or less on to glass or quartz substrates held at room temperature (RT), using an Edwards coater unit type E306A. The film thickness was controlled using a thickness monitor and then measured applying the interferometric method of Tolansky. X-ray diffraction of a Philips diffractometer with a  $\text{CuK}\alpha$  source, differential thermal analyser (Shimadzu DT-30) and metallurgical microscope, were used to identify the amorphous structural nature of the prepared films.

The spectral distribution curves of the transmittance ( $T$ ) and the reflectance ( $R$ ) have been recorded for the deposited selenium films using both a spectrophotometer (Model Varian Cary 2390) and a specially constructed temperature-controlled optical system [9]. The latter gave very promising data for the distribution curves, mainly in the spectrum of the absorption range (400 to 720 nm). The transmittance was measured at nearly normal incidence. The reflectance was measured by rotating the sample film vertically around the axis of the specimen holder where the angle between the incident monochromatic light and the normal to the surface of the sample did not exceed 8°.

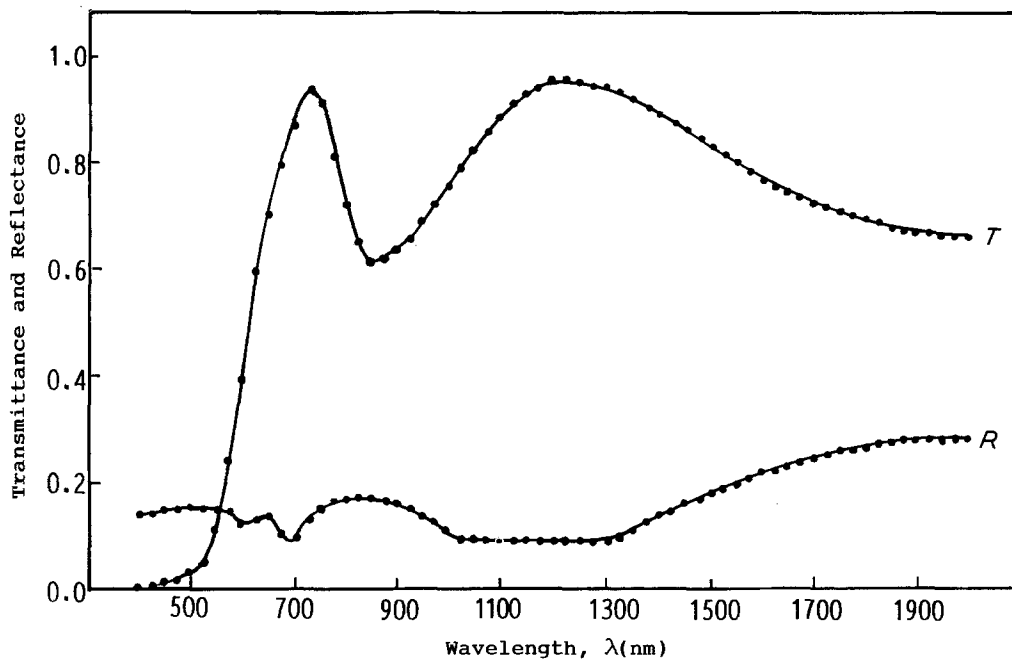


Figure 1 The spectral distribution curves of  $T$  and  $R$  for a-Se film of thickness 450 nm.

Hadley's spectrophotometric method [10] is applied to calculate the refractive ( $n$ ) and absorption ( $k$ ) indices from the experimental data of  $T$  and  $R$  using the computer facilities (Apple-Mackintosh, 128 K byte) in our laboratory.

### 3. Results and discussion

#### 3.1. Effect of a-Se film thickness on $T$ and $R$

Three different values of thickness ( $d$ ), namely 321.2, 450, 515.7 nm, of a-Se were deposited on quartz substrates by the thermal evaporation technique. Fig. 1 shows the spectral distribution curves of a-Se film of  $d = 450$  nm, as an example. The measurements of  $T$  and  $R$  were carried out at normal incidence and at RT in the spectrum range 400 to 2000 nm using the spectrophotometer. The figure shows that  $T$  is always

higher than  $R$  at any wavelength,  $\lambda$ , which is also the case in the two other thicknesses investigated. The absorption range is limited to 580 to 720 nm (depending on  $d$ ), after which the variation of  $T$  and  $R$  are opposite in an oscillatory form. The oscillation in  $T$ ,  $R = f(\lambda)$  is minimum when  $d = 450$  nm. Also, for this thickness, the relative variation of  $T$  is maximum in the absorption range 400 to 720 nm.

For the data of the optical system, the intensity of the transmitted light from the sample is  $I_0 I_f T_s$ , where  $I_0$  is the intensity of the incident light at a particular  $\lambda$  and  $I_f$  is the transmission through the film only. The transmission through the substrate,  $T_s$ , was recorded by using a blank substrate as a reference material. The same process is considered for the case of reflection where the reference is a highly reflective silver mirror. Fig. 2 shows the variation of  $T$  in the absorption range for a-Se films of 450 nm deposited on glass and quartz substrates obtained by using the constructed optical system together with the spectrophotometer data. The agreement shown in the figure between the different data is also valid for the other two thicknesses investigated.

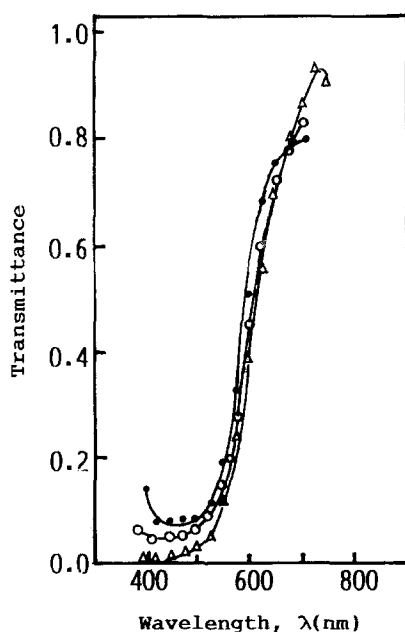


Figure 2 The spectral distribution curves of  $T$  for a-Se film of thickness 450 nm deposited on (O) glass and quartz using: (●) constructed optical system and ( $\Delta$ ) spectrophotometer.

#### 3.2. The wavelength dependence of $n$ and $k$

Fig. 3 shows variation of the functions  $n, k = f(\lambda)$  for the three thicknesses of the a-Se films investigated. Here, it is worth noting that the error in determining  $n$  over the whole range of the spectrum presented in the applied method does not exceed 1%, while the error in determining  $k$  is increased to 5%. For a-Se of 450 nm, the wavelength dependence of  $n$  and  $k$  is represented in the figure for the data obtained by using both the spectrophotometer and the constructed optical system.

#### 3.3. The optical energy gap of a-Se

The value of  $E_g^{opt}$  can be calculated from the general equation adopted by Hasegawa *et al.* [11]. This equation relates the absorption coefficient ( $\alpha$ ) to the

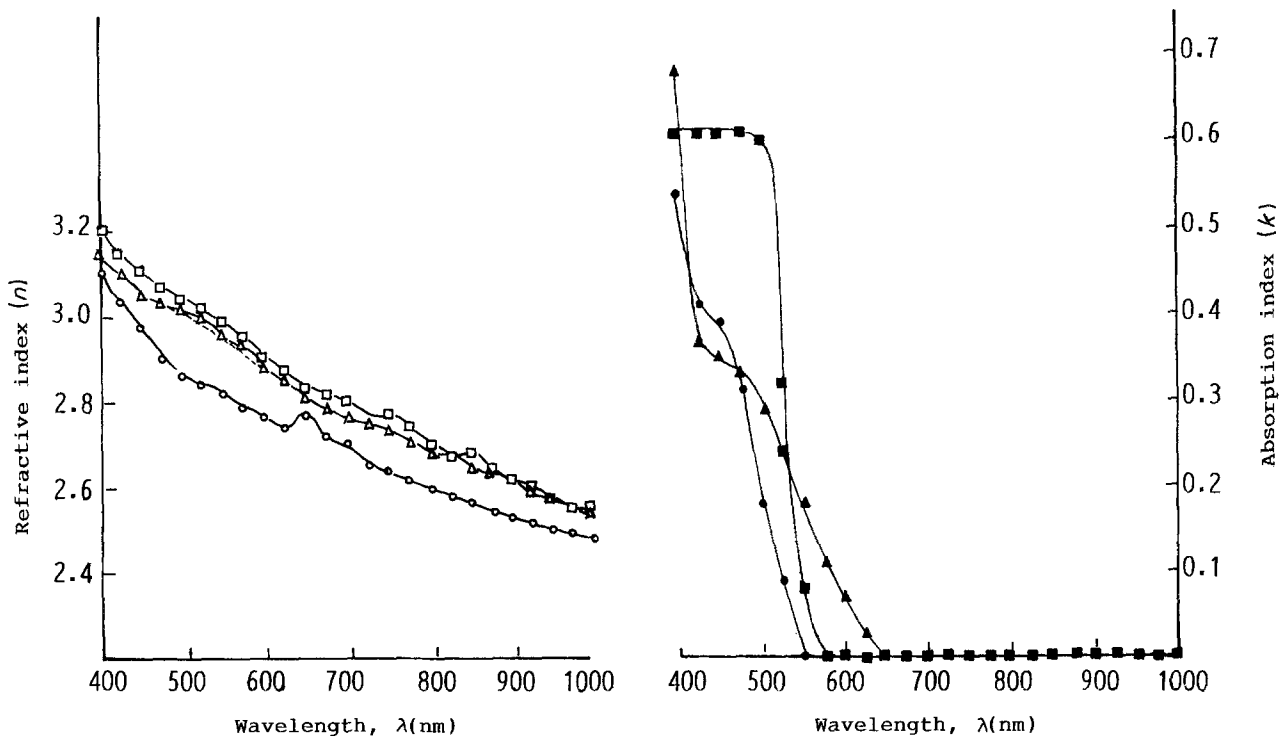


Figure 3 The wavelength dependence of (○, △, □)  $n$  and (●, ▲, ■)  $k$  for a-Se films of different thicknesses. (---) Data obtained from the constructed optical system for thickness 450 nm.  $d =$  (○, ●) 321.2 nm, (△, ▲) 450 nm, (□, ■) 515.7 nm.

optical gap of amorphous solids

$$(\hbar\omega\alpha)^n = B(\hbar\omega - E_g^{\text{opt}}) \quad (1)$$

where  $n = \frac{1}{2}$  [12] or  $n = 1$  [13], and  $B$  is a constant. The optical absorption coefficient can be calculated from the equation

$$\alpha = t^{-1} \ln(I_0/I) \quad (2)$$

The quantities  $(\hbar\omega\alpha)$  and  $(\hbar\omega\alpha)^{\frac{1}{2}}$  have been plotted as a function of the incident photon energy ( $\hbar\omega$ ) for the deposited different thicknesses of a-Se films and the results are given in Fig. 4. The linear parts of the curves in the lower energy region are found to follow the following two sets of equations which are obtained

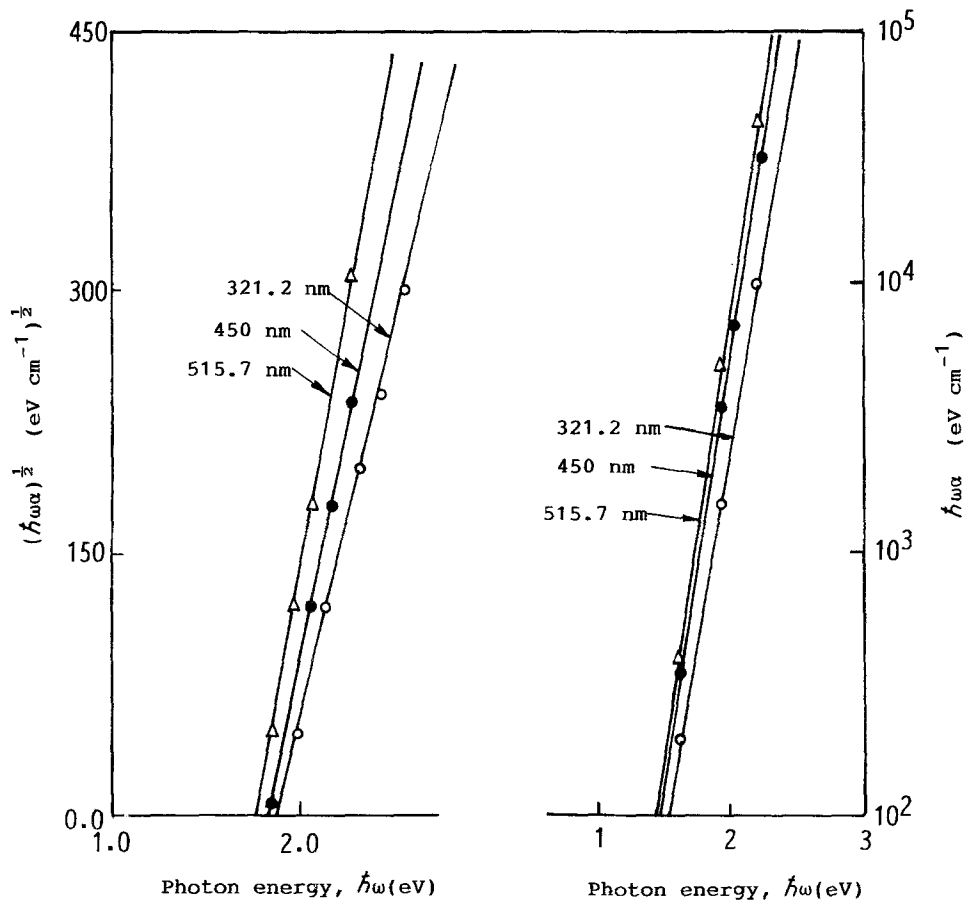


Figure 4 The photon energy dependence of  $(\hbar\omega\alpha)^{\frac{1}{2}}$  and  $\hbar\omega\alpha$  for a-Se films of different thicknesses.

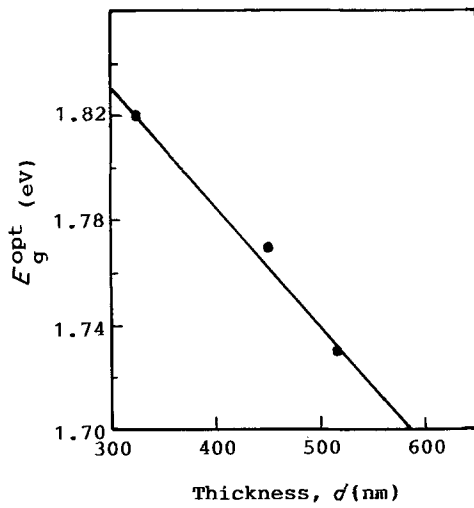


Figure 5 Optical energy gap dependence of a-Se thickness (Equation 1,  $n = \frac{1}{2}$ ).

by applying the method of least squares

$$\begin{aligned} (\hbar\omega\alpha) &= 22\,500(\hbar\omega - 1.52), & \text{for } t = 321.2 \text{ nm} \\ (\hbar\omega\alpha) &= 20\,000(\hbar\omega - 1.45), & \text{for } t = 450 \text{ nm} \\ (\hbar\omega\alpha) &= 10\,000(\hbar\omega - 1.43), & \text{for } t = 515.7 \text{ nm} \end{aligned} \quad (3)$$

and

$$\begin{aligned} (\hbar\omega\alpha)^{1/2} &= 480(\hbar\omega - 1.82), & \text{for } t = 321.2 \text{ nm} \\ (\hbar\omega\alpha)^{1/2} &= 660(\hbar\omega - 1.77), & \text{for } t = 450 \text{ nm} \\ (\hbar\omega\alpha)^{1/2} &= 720(\hbar\omega - 1.73), & \text{for } t = 515.7 \text{ nm} \end{aligned} \quad (4)$$

By comparing these two sets of equations with

TABLE I The optical energy gap of a-Se films of different thicknesses

Film thickness (nm)	$E_g^{\text{opt}}$ (eV) (Eqn 1)	
	when $n = \frac{1}{2}$	when $n = 1$
321.2	1.82	1.52
450	1.77	1.45
515.7	1.73	1.43

Equation 1, the values of  $E_g^{\text{opt}}$  are estimated and given in Table I. These values for a-Se corroborate the results obtained by others [12–14].

Fig. 4 shows that the absorption edge is shifted to lower photon energies with increasing film thickness. Also, a-Se films display a decrease of optical gap with an increase of thickness of the film. Increasing  $d$  from 321.2 to 515.7 nm is accompanied by a decrease in  $E_g^{\text{opt}}$  from 1.82 to 1.73 eV when  $n = \frac{1}{2}$ , and a decrease from 1.52 to 1.43 eV when considering  $n = 1$  in Equation 1. The last condition assumes one-dimensional chain structure of selenium which could not be the exact situation for selenium films having a thickness higher than 200 nm.

Considering  $n = \frac{1}{2}$ , Fig. 5 shows the  $d$  dependence of  $E_g^{\text{opt}}$  for a-Se. This figure indicates that such a dependence is nearly linear with a slope of  $5 \times 10^{-4} \text{ eV nm}^{-1}$ .

### 3.4. Isothermal time dependence of $T$ , $R$ , $n$ and $k$

The quantities  $T$  and  $R$  are considered as structure-sensitive parameters to follow the crystal growth in a-Se films. The measurements were taken using a

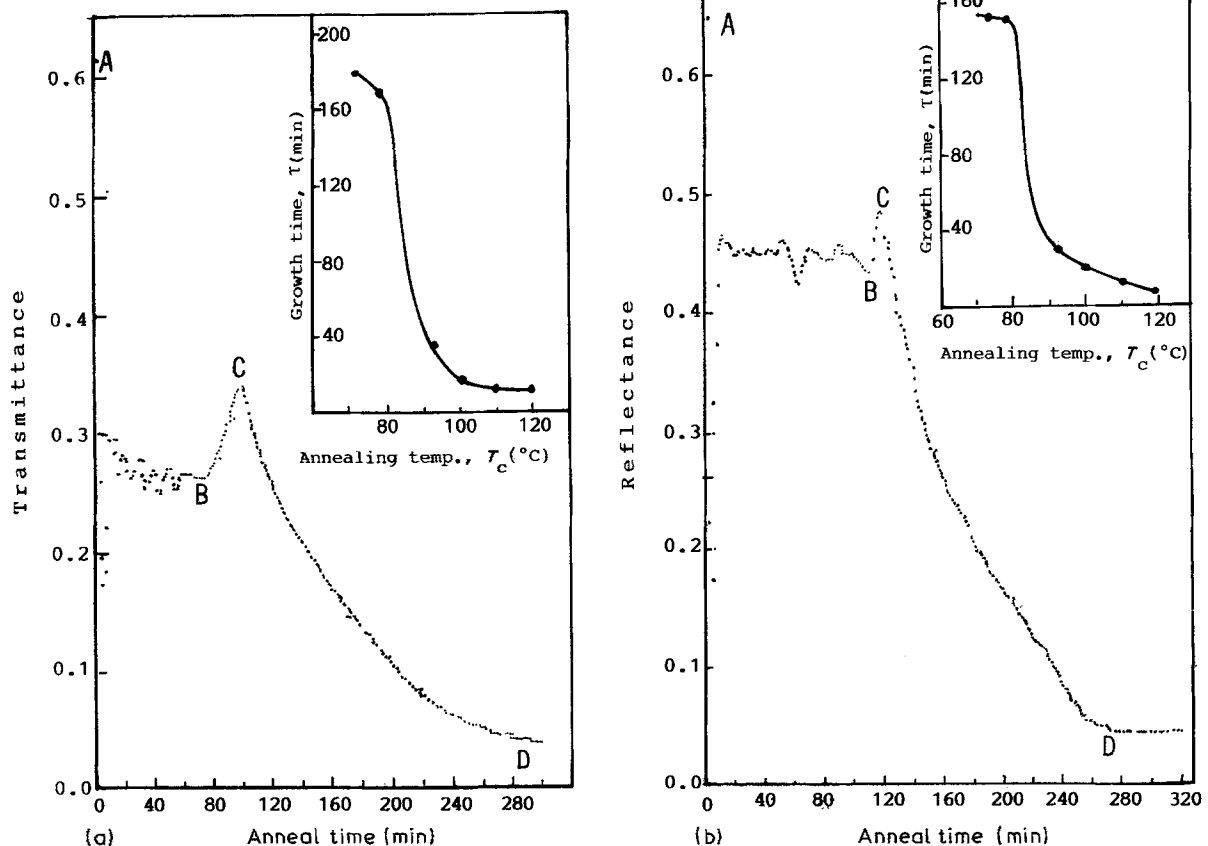


Figure 6 Time dependence of (a) reflectance and (b) transmittance of a-Se film of 450 nm annealed at 70°C and 700 nm. The insets give the temperature dependence of the growth time ( $\tau$ ).

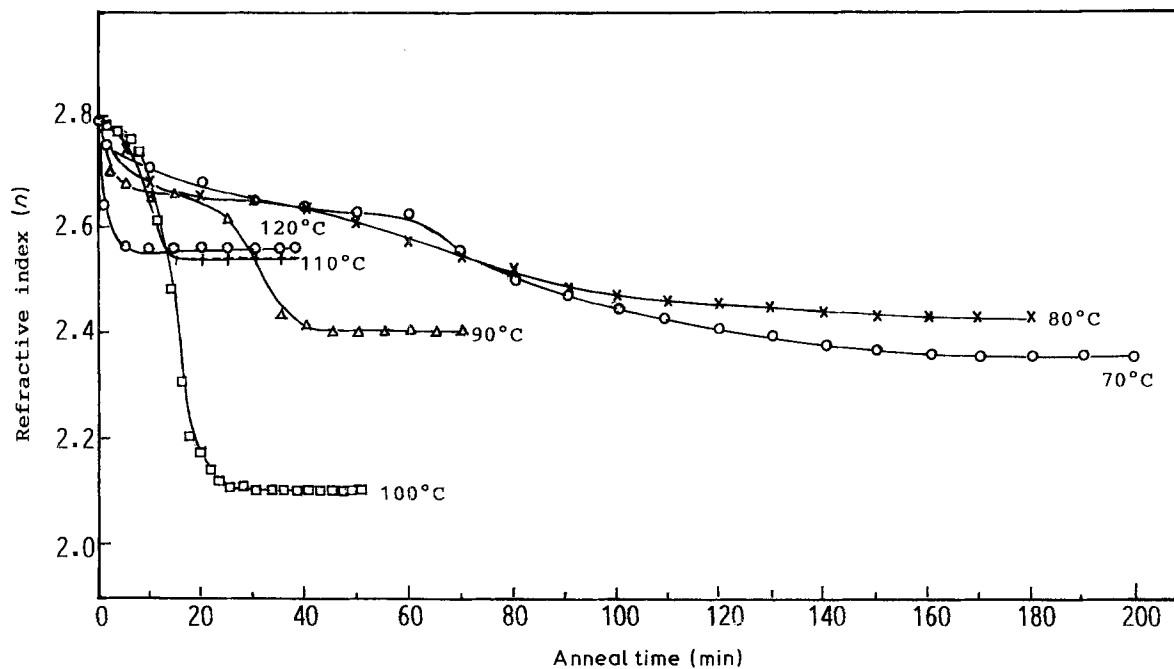


Figure 7 Isothermal time-dependence of the refractive index during the growth stage of a-Se films of thickness 450 nm at different isotherms during the incidence of isoenergetic photons of energy 1.8 eV.

technique [9] developed especially for recording the continuous relative variation of  $T$  and  $R$  (1 min intervals) at different isotherms in the temperature range 70 to 120°C. A monochromatic wavelength of 700 nm was selected for the incident photons during all the measurements. This wavelength corresponds to a rela-

tively maximum value for both  $T$  and  $R$  when  $d = 450$  nm and lies in the absorption range of a-Se.

Fig. 6 shows the time-dependence of both  $T$  and  $R$  for a-Se films of  $d = 450$  nm isothermally annealed at 70°C during the incidence of isoenergetic photons of  $\lambda = 700$  nm. Such a variation of  $T$  or  $R$  corresponds

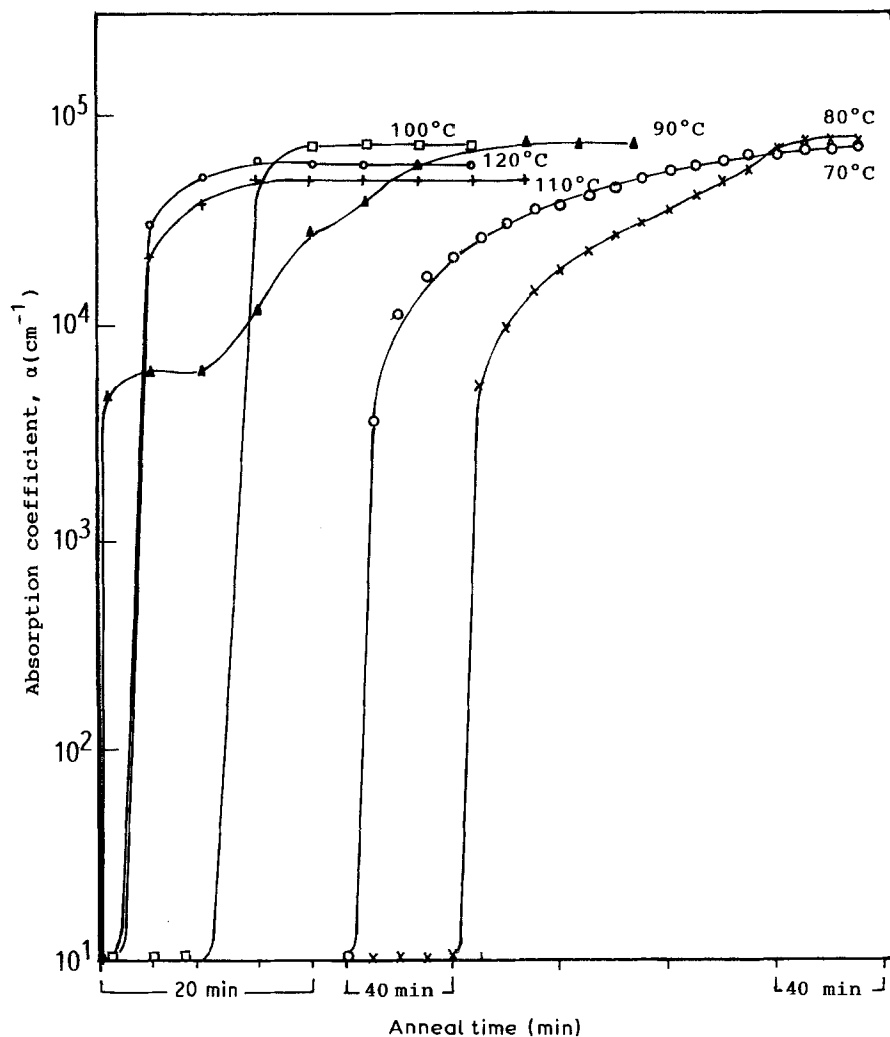


Figure 8 Isothermal time-dependence of the absorption coefficient of a-Se films of thickness 450 nm crystallized at different isotherms during the incidence of isoenergetic photons of energy 1.8 eV.

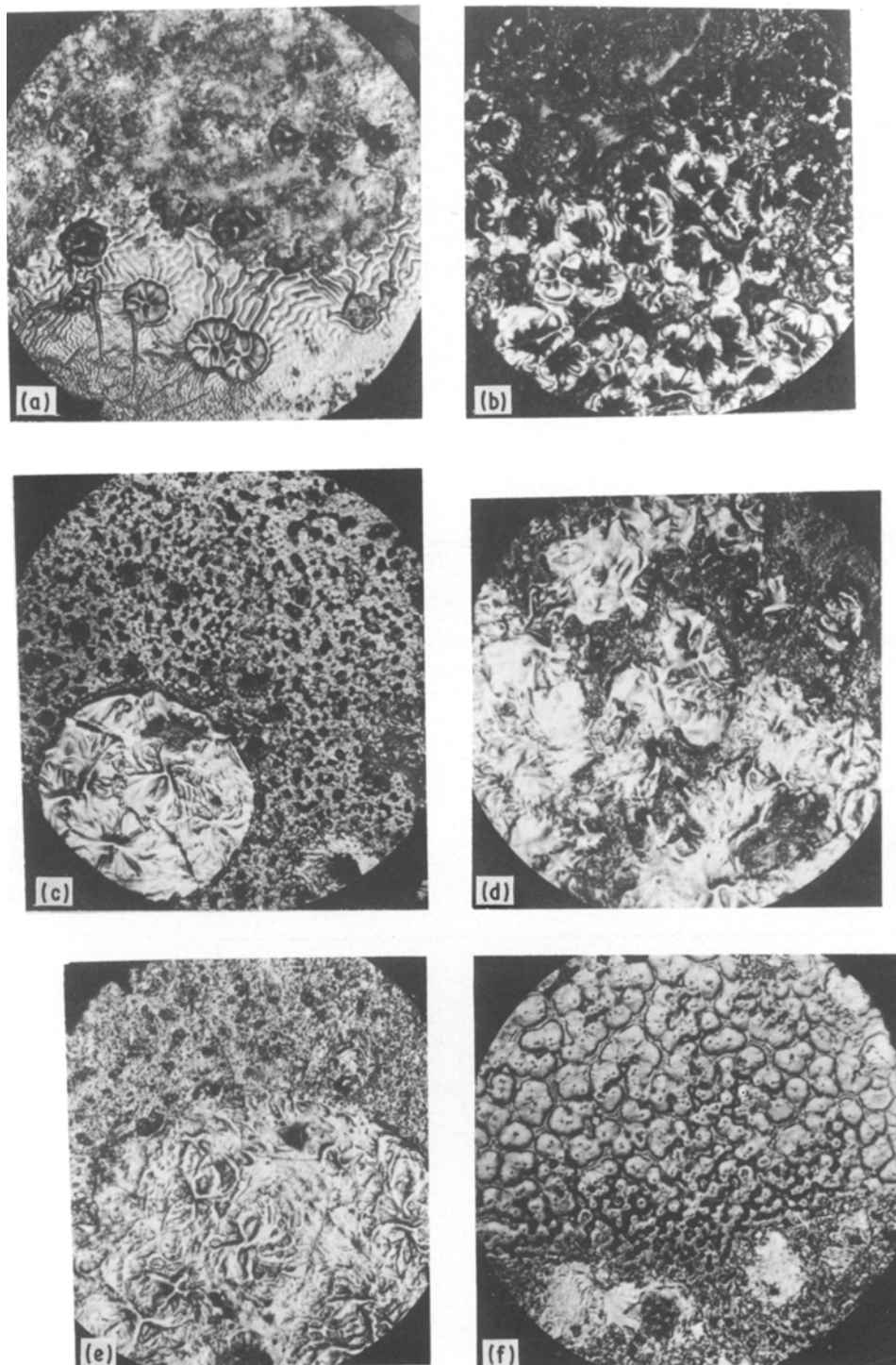


Figure 9 Reflection micrograph patterns of a-Se crystallized at different isotherms.  $X = 350$ . (a) 70°C, (b) 80°C, (c) 90°C, (d) 100°C, (e) 110°C, (f) 120°C.

to a transition from the amorphous (a) to the crystalline (c) state. In the figure, the transition a-c passes via three different time-dependent stages. These stages may be defined as follows.

(i) Region AB; indicates fast and irregular changes in  $T$  and in  $R$  due to random scattering of the incident photons in the metastable a-Se matrix. The scattering of points in this stage is a result of the normal heating of the amorphous film from RT to the preheated oven temperature of annealing, 70°C.

(ii) Region BC; where there is a small regular increase in  $T$  or in  $R$  with time of annealing.

(iii) Region CD; where there is a gradual decrease in

$T$  as well as in  $R$  with the annealing time. Such a smooth decrease is associated with the transformation from non-equilibrium thermodynamic state of high  $T$  and  $R$  to a rather equilibrium one with lower  $T$  and  $R$ . The value of both  $T$  and  $R$  reaches a limiting constant value at points D.

Similar behaviour to that in Fig. 6 has been observed for the other values of  $T_c$ . Increasing  $T_c$  leads to a decrease in the total time necessary for completing the a-c transformation process, as well as in the time of the individual stages.

The constancy of the minimum limiting value of  $T$  or  $R$  which was attained at a given  $T_c$  indicates the

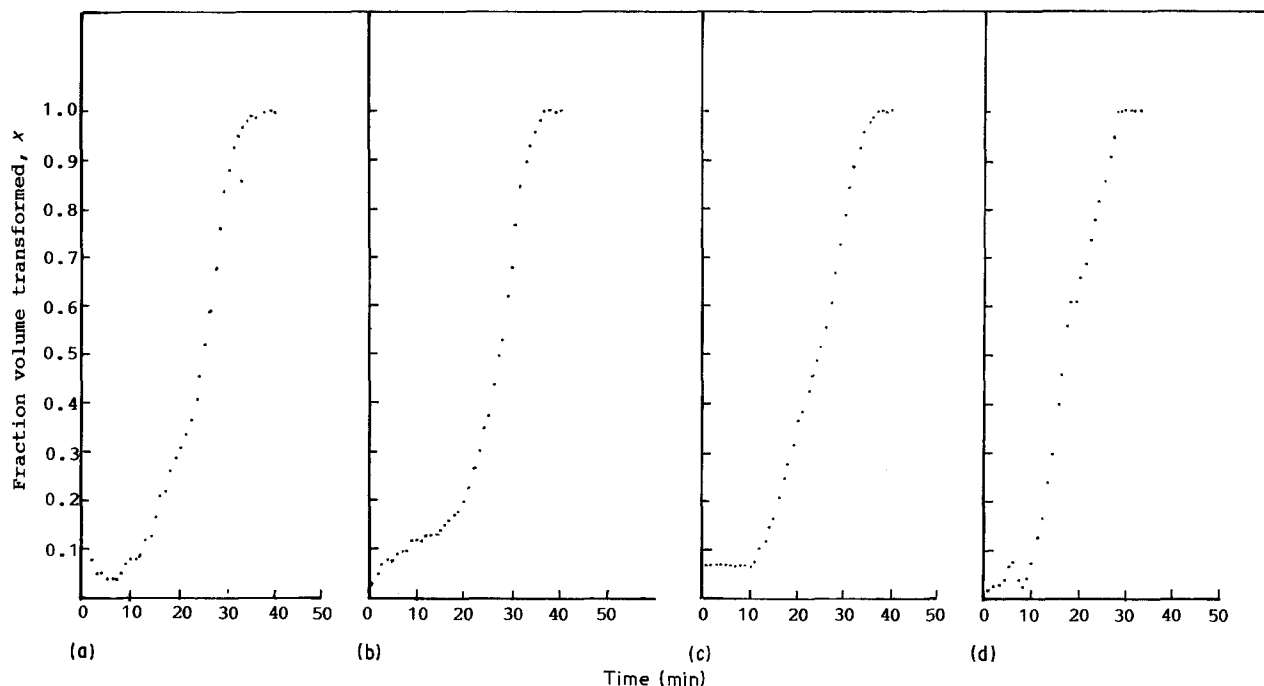


Figure 10 The time-dependence of the transformed fraction; for a-Se films of thickness 450 nm crystallized at 90°C, as calculated according to different optical quantities: (a)  $R$ , (b)  $n$ , (c)  $\alpha$  and (d)  $T$ .

completion of the possible transformation process in the film investigated. The variation of the limiting value with  $T_c$  is mainly due to the degree of structural perfection attained at this condition of annealing.

The continuous variation in values of the optical indices  $n$  and  $k$  during the growth stages (regions CD in Fig. 6) has been calculated at the different isotherms investigated using the curves of  $T$ ,  $R = f(t)$  by applying Hadley's method. Figs 7 and 8 show, respectively, the isothermal time-dependence of the optical constants  $n$  and  $\alpha (= 4\pi k/\lambda)$  for a-Se films of thickness 450 nm isothermally annealed at different temperatures under the incidence of isoenergetic photons of energy 1.8 eV. The figures indicate a gradual decrease in  $n$  and increases in  $\alpha$  during the growth stage until they approach constant values with change in  $T_c$ . The abrupt increase in the absorption from a minimum value to a certain value after which the absorption increases gradually reaching a maximum limiting value, corresponds to the crystallized stage. The latter lies in the region on  $5 \times 10^5 \text{ cm}^{-1}$ .

### 3.5. Microstructural investigation of selenium films

Normally, selenium crystallization [15, 16] proceeds via the formation of spherulites having a lamellar structure with the width of the lamellae much less than the length of the extended selenium chain. This accommodation of the selenium chain is affected by the repeated folding of the chains, giving rise to spherulites having a series of concentric rings.

A spherulite is a spherically symmetrical formation made of radial rays diverging from the centre. The simplest structural elements in a spherulite, like spherulites themselves, are interconnected by a large number of interstructural bonds in the form of the macromolecules, bundles of macromolecular or crystallized lamellar formations made mainly out of

chains in an extended conformation. Such bonds are formed if several macromolecules begin to crystallize simultaneously from both ends in various crystallites which are in the same spherulite or even in different spherulites. This is possible owing to a very weak correlation of the motion of the chain segments which are very far away. Such interstructural bonds combine both separate crystallites inside the lamellae.

In the present work, the optical microscopy technique was used to record the crystallized structure of the selenium films after subjecting them to isothermal annealing corresponding to the limiting constant value (points D on Fig. 6) at each temperature. Fig. 9 shows such reflection micrograph patterns recorded at

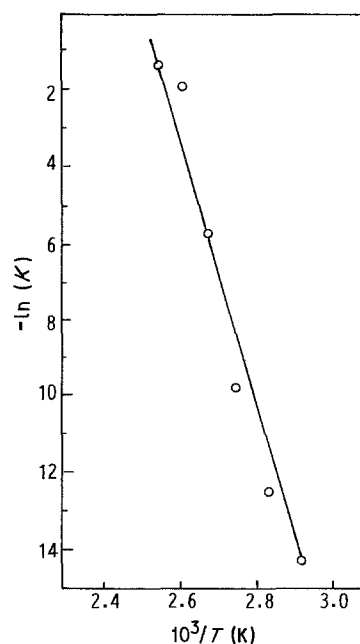


Figure 11 Relation between  $\ln(K)$  and  $1/T(K)$  for selenium films of thickness 450 nm.

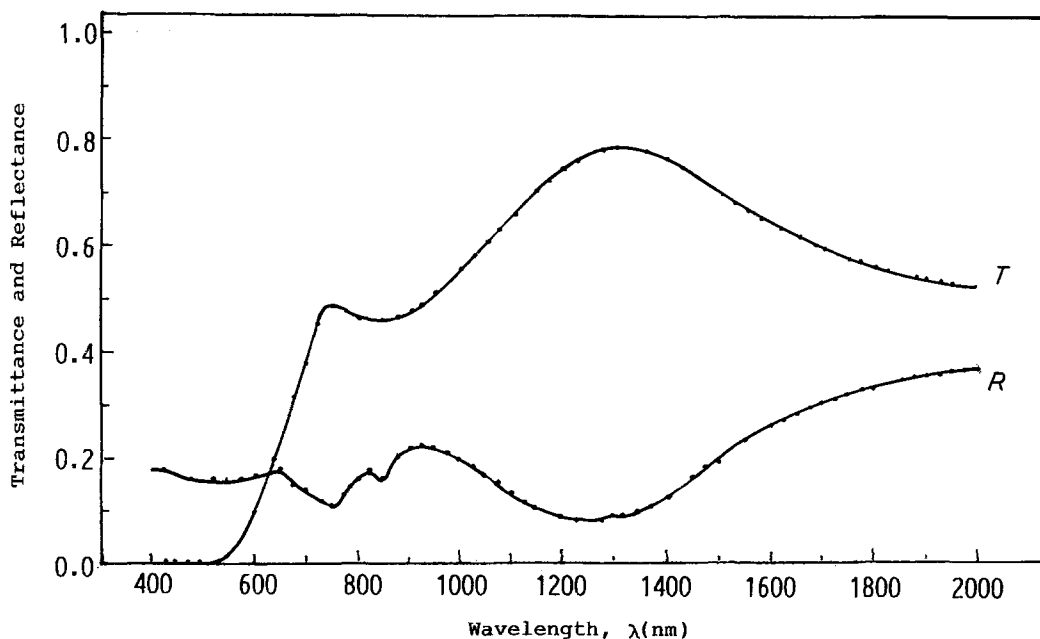


Figure 12 The spectral distribution curves of  $T$  and  $R$  for selenium films of thickness 450 nm crystallized at 100°C.

the end of each annealing temperature investigated in the range 70 to 120°C. These micrographs show different morphologies of crystallization for the different temperatures of annealing. These morphologies are matched with the foregoing explanation of the crystallization process of amorphous selenium. That is, the crystallization process starts at small centres randomly distributed in the amorphous medium. These centres are gradually increased in size by increasing the crystallization time. It is also found that the spherulites can swallow each other during the growth process as their numbers obviously decrease with increasing annealing time. Also, the beginning of the formation of lamellae is observed in the micrograph at low temperature (70°C), and the formation of spherulites is observed in the micrograph at relatively high temperature (e.g. 120°C). Of course, the annealing temperature plays another role in controlling the rate of crystal growth, as is clear from the different textures of selenium crystallized at different isotherms in Fig. 9. There are, however, some portions where crystallization has not yet taken place. These regions are still amorphous, and almost decreased with increasing annealing temperature. It is worth noting that the limiting stages of the crystallization morphology observed in the figure are related to the time of annealing considered. The latter is in accordance with the data given in the insets of Fig. 6.

### 3.6. Kinetics of isothermal crystallization

At any intermediate stage in the a-c transformation, the material contains the two phases that exist simultaneously. The concentration of each may be defined as the volume part relative to an overall volume of unity. That is, to study the kinetics of transformation, the experimental data of  $T$ ,  $R$ ,  $n$ ,  $\alpha = f(t)$  should be expressed in terms of the transformed fraction  $x = (1 - \theta)$  at different crystallization time.  $\theta$  represents the untransformed fractional volume.

In this respect, the fractional transformed volume

can be calculated from an empirical relation in the form [17]

$$[1 - x(t)] = \theta(t) = (H_{\infty} - H_t)/(H_{\infty} - H_0)$$

where  $H$  is a structure-sensitive parameter following the a-c transformation. The subscripts  $\infty$  and 0 represent the values of the considered parameter ( $T$ ,  $R$ ,  $n$  or  $\alpha$ ) at the final (point D) and the initial (point C) modes, and ( $t$ ) is that at the intermediate (growth) state.

The plots of  $x = (1 - \theta)$  against annealing time ( $t$ ) give a measure of the rate of crystal growth and also an idea about the uniformity of the crystallization process. Typical curves of such plots are given in Fig. 10 for a-Se films of thickness 450 nm crystallized at 90°C, as an example. The figure indicates that the functions  $x(T, R, n \text{ or } \alpha) = f(t)$  are almost sigmoidal in shape, indicating an autocatalytic reaction as is often observed in various kinds of solid reactions. For any of these functions, the crystallization rate curves appear to shift towards lower time scales with increasing temperature, as one might expect from the decrease in viscosity with increasing  $T_c$ .

Analysis of the crystallization process has been carried out using the Avrami equation [18-20]

$$x(t) = 1 - \exp(-Kt^m).$$

where  $K$  is a function of temperature and generally depends on both the nucleation rate and the growth rate,  $m$  is a parameter which reflects the nucleation

TABLE II The temperature dependence of the Avrami constants  $m$  and  $K$  for selenium films of thickness 450 nm

Cryst. temp. (°C)	$m$	$-\ln(K)$
70	2.7	14.30
80	2.4	12.51
90	2.2	9.79
100	2.0	5.68
110	1.4	1.90
120	1.5	1.50



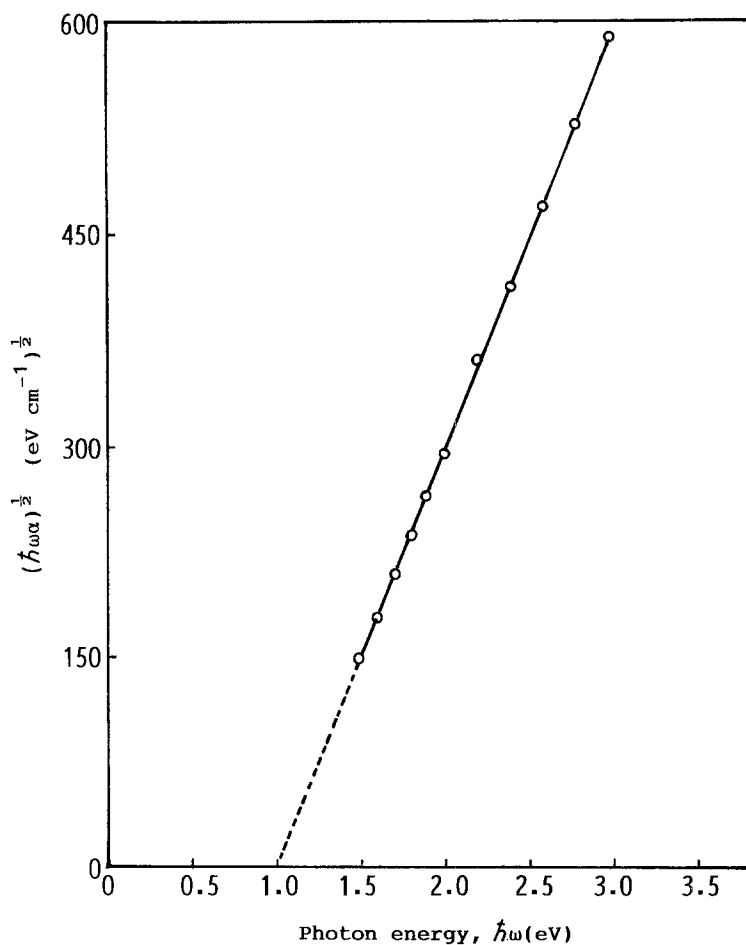


Figure 13 The photon energy dependence of  $(\hbar\omega\alpha)^{1/2}$  for selenium film of thickness 450 nm crystallized at 100° C.

rate and/or the growth morphology of the material. To fit the Avrami equation, a plot of  $\ln[-\ln(1-x_t)]$  against  $\ln(t)$  must yield a straight line whose slope is  $m$  and whose intercept on the ordinate at  $\ln(t) = 0$  is  $\ln(K)$ . This has been verified for the investigated selenium films during the transformation process over the investigated temperature range, 70 to 120° C. The results of  $m$  and  $K$  are given in Table II as a function of  $T_c$ .

The values obtained for the Avrami exponent  $m$  are in good agreement with those obtained for selenium on the basis of the changes in the dielectric constant ( $\epsilon$ ) with time of crystallization [21]. Fractional values of the experimentally obtained  $m$  can be theoretically explained by Evan's principle [22], suggesting a linear change in the number of nuclei with time. The decrease of  $m$  with increasing temperature may indicate that the crystallization process is of predetermined growth type.

A plot of  $\ln(K)$  against  $1/T$  yields a straight line defining the activation energy of crystallization,  $E$ , according to the formula

$$K = K_0 \exp(-E/RT)$$

where  $R$  is the universal gas constant. Fig. 11 shows such a plot for the selenium films investigated. The value of  $E$  is found to be 1.3 eV in the temperature range investigated. This value is in good agreement with those obtained for selenium using different techniques [21, 23, 24].

### 3.7. Optical energy gap of a-Se

Fig. 12 shows the spectral distribution curves of  $T$  and

$R$  for a-Se film of thickness 450 nm crystallized at 100° C. As in the case of amorphous films, Hadley's spectrophotometric method is applied to calculate the optical constants. The values of the absorption coefficient ( $\alpha$ ) are used to calculate the optical energy gap  $E_g^{\text{opt}}$  for the crystallized selenium film. The results are given in Fig. 13, where the value of  $E_g^{\text{opt}}$  is found to be 1.0 eV. This value is decreased more than that for the amorphous film by 56% (Table I).

### References

1. P. SELENYI, *Nature* **161** (1948) 522.
2. *Idem*, *Acta Phys.* **2** (1952) 129.
3. N. FURUTRA, *J. Sci. Hiroshima Univ.* **24** (1960) 328.
4. M. A. TAKIBI and T. M. VERDIENA, "Selenium, Tellurium and their Applications", (Acad. Sci. Azerbaijan USSR, Baka, 1965).
5. J. DRESNER and G. B. STRINGFELLOW, *J. Phys. Chem. Solids* **29** (1968) 303.
6. S. R. OVSHINSKY and P. H. KLOSE, *Digest Techn. Papers* (1971) p. 58.
7. M. F. KOTKATA, F. M. AYAD and M. K. ELMOUSLY, *J. Non-Cryst. Solids* **33** (1979) 13.
8. S. R. OVSHINSKY and D. ADLER, *Contemp. Phys.* **19** (1978) 109.
9. F. A. ABDEL-WAHAB, MSc thesis, Ain Shams University (1987).
10. L. N. HADLEY, cited by Heavens, in "Physics of Thin Films", edited by G. Hass and R. E. Thon, Vol. 2 (Academic, New York, 1964) p. 193.
11. S. HASEGAWAA, S. YAZAKI and T. SHIMIZU, *Solid State Commun.* **26** (1978) 4070.
12. S. CHAUDHURI, S. K. BISWAS, A. CHOUDHURY and K. GOSWAMI, *J. Non-Cryst. Solids* **46** (1981) 171.
13. S. K. J. AL-ANI and C. A. HOGARTH, *ibid.* **69** (1984) 167.

14. J. P. AUDIERE, CH. MAZIERES and J. C. CARBALIES, *ibid.* **27** (1978) 411.
15. A. TAGER, "Physical Chemistry of Polymers", 2nd Edn (Mir, Moscow, 1978).
16. R. A. WESTBURY and W. C. COOPER, in "Selenium", edited by R. A. Zingaro and W. Cooper, (Van Nostrand-Reinhold, New York, 1979).
17. M. F. KOTKATA and K. M. KANDIL, *Mater. Sci. Engng* **95** (1987) 287.
18. M. AVRAMI, *J. Chem. Phys.* **7** (1939) 1103.
19. *Idem, ibid.* **8** (1940) 212.
20. *Idem, ibid.* **9** (1941) 177.
21. M. F. KOTKATA, H. A. KHALEK, W. M. ATIA, T. PORJESZ and M. EL-SAMAHY, *J. Mater. Sci.* **20** (1985) 2973.
22. U. R. EVANS, *Trans. Faraday Soc.* **41** (1945) 365.
23. M. F. KOTKATA and M. K. EL-MOUSLY, *Acta Phys. Hung.* **54** (1983) 303.
24. M. F. KOTKATA, M. H. EL-FOULY, A. Z. EL-BEHAY and L. A. EL-WAHAB, *Mater. Sci. Engng* **60** (1983) 163.

*Received 13 November 1987  
and accepted 3 March 1988*